

Title	FEM Analysis of 3-D Welding Residual Stresses and Angular Distortion in T-type Fillet Welds(Mechanics, Strength & Structural Design)
Author(s)	Ma, Ning Xu; Ueda, Yukio; Murakawa, Hidekazu; Maeda, Hideaki
Citation	Transactions of JWRI. 24(2) P.115-P.122
Issue Date	1995-12
Text Version	publisher
URL	<a href="http://hdl.handle.net/11094/5911">http://hdl.handle.net/11094/5911</a>
DOI	
rights	本文データはCiNiiから複製したものである
Note	

***Osaka University Knowledge Archive : OUKA***

<https://ir.library.osaka-u.ac.jp/repo/ouka/all/>

## FEM Analysis of 3-D Welding Residual Stresses and Angular Distortion in T-type Fillet Welds †

Ning-Xu MA\*, Yukio UEDA\*\*, Hidekazu MURAKAWA\*\*\*  
and Hideaki MAEDA\*\*\*\*

### Abstract

*In this paper, the residual stresses in T-type fillet welds are computed by thermal elastic plastic three dimensional FEM and generalized plane strain FEM. Then the residual stresses and their distribution patterns in single pass and multipass T-type fillet welded joints are clarified. From the analyzed results, it is observed that a large tensile transverse residual stress is produced near the fillet toe, which has a very detrimental effect on fatigue cracking. The tensile transverse residual stress near a multipass fillet weld toe is larger than that near the single pass fillet weld toes, and it is mainly induced by the two welding passes close to the fillet toe. Furthermore, the effects of welding sequence, welding penetration, heat input, plate thickness and restraint conditions on the tensile transverse residual stress are investigated. With increasing welding heat input or penetration, the tensile transverse residual stress decreases. With increasing flange thickness, the tensile transverse residual stress increases. When the flange is restrained during welding and the restraint force is released after welding, the tensile transverse residual stress near the fillet toe can be reduced. In the last section, the angular distortion in T-type fillet welds is computed by generalized plane strain FEM, and the effect of the welding sequence, the support of working table and the applied external restraint position are investigated*

**KEY WORDS:** (FEM) (3-D) (Generalized Plane Strain) (Residual Stresses) (Angular Distortion) (T-type Fillet Welds) (Weld Toes) (Single Pass Welding) (Multipass Welding) (Welding Sequence) (Welding Penetration) (Restraint Conditions)

### 1. Introduction

Transient and residual welding stresses are very important in the evaluation of weldability. During these 20 years, many computations and measurements have been made on the welding stresses in butt welded joints<sup>1-6)</sup>, only a few researches have been conducted on fillet welded joints<sup>7-9)</sup>. Fillet joints are widely used in ship and bridge structures. In this paper, the authors take the T-type fillet welded joint as a typical example.

Firstly, the three dimensional stresses in T-type fillet joints are analyzed using the elastic plastic three dimensional FEM (3-D FEM). Then, the generalized plane strain FEM model is employed and its accuracy is verified by comparing computed welding residual stresses with those computed by 3-D FEM. With the aid of the generalized plane strain FEM modelling, the residual stresses and their distribution characteristics in the single-pass and multipass T-type fillet welds are analyzed. Furthermore, the effects of welding sequence, welding penetration, heat input, plate thickness and restraint conditions on the transverse residual stresses near the fillet weld toes, which has a large effect on fatigue

cracking<sup>10,11)</sup>, are investigated.

### 2. 3-D FEM Modelling and Residual Stresses in T-type Fillet Welds

#### 2.1 3-D FEM Modelling

The three dimensional FEM model of a fillet weld used in the stress analysis is shown in Fig. 1. For the T-type fillet weld, the two welds at the two sides of the web are assumed to be simultaneously welded with the same welding conditions. Therefore, the T-type fillet weld can be considered to be symmetric with x-z plane. Using this symmetric condition, only half of the T-type fillet weld shown in Fig. 1 is taken and meshed in the FEM analysis. As shown in Fig. 1, the length of the fillet weld, the half width of the flange and the height of the web are assumed to be 500 mm, 100 mm and 30 mm, respectively. The plate thickness is 20 mm for the flange and 8 mm for the web. The fillet size is 6 mm. The welding conditions used in the analysis are also shown in Fig. 1. The effective heat input for unit weld length is 840 (J/mm) if the welding heat efficiency is assumed to be 60% in the analysis.

† Received on Nov. 24, 1995

\* Research Associate

\*\* Professor

\*\*\* Associate Professor

\*\*\*\* Engineer, Mitsubishi Electric Ltd

Transaction of JWRI is published by Welding Research Institute of Osaka University, 11-1, Mihogaoka, Ibaraki, Osaka 567, Japan.

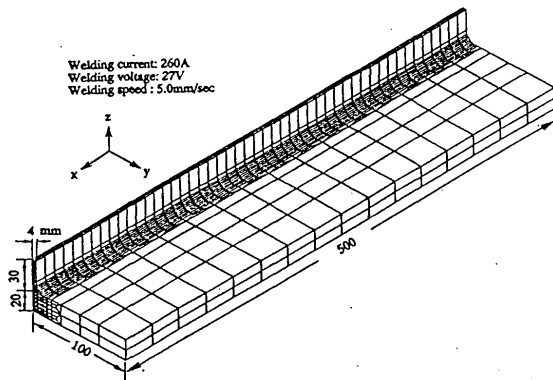


Fig. 1 3-D Mesh division for T-type Fillet Weld

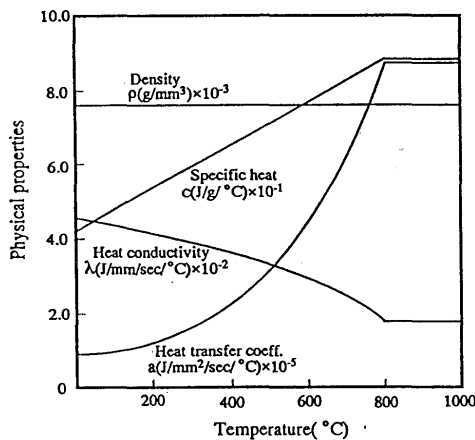


Fig. 2 Physical properties of steels

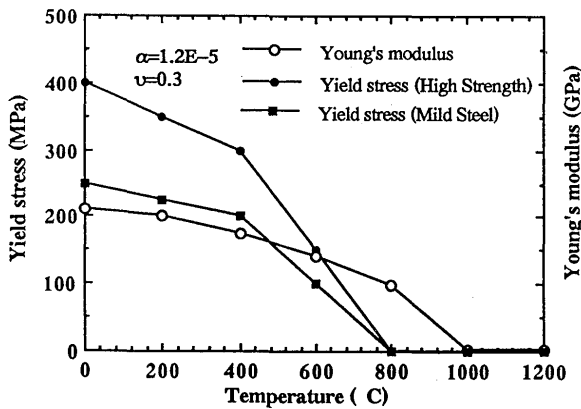


Fig. 3 Mechanical properties of high strength steel and mild steel

The material used in the three dimensional FEM analysis for residual stresses is assumed to be high strength steel. The physical properties of steels and their temperature dependency used in welding heat conduction FEM analysis are shown in Fig. 2. The Young's modulus, yield strength and their temperature dependency are shown in Fig. 3. In Fig. 3, the yield strength of mild steel and its temperature dependency is also shown, since this will be used later. As shown in Fig. 3, the

mechanical melting temperature of the steels is assumed to be 800°C. The thermal expansion coefficient  $\alpha$  of steels is assumed to be constant. It is also assumed that the weld metal, the HAZ and the base metal have the same properties.

In the thermal elastic-plastic FEM analysis, the elements are divided into three types. The first type is the elements to be welded which do not exist before welding and appear after weld metal starts solidification. The second type is the elements whose maximum temperature in thermal cycles is more than the mechanical melting point. When the temperature exceeds the mechanical melting point, plastic strain and stress are set to be zero since the material loses its resistance to deformation. The elements for tack welds also belong to this type. The third type are the general elements of base metal which undergo relatively lower temperature thermal cycles.

## 2.2 Residual Stresses and Strain in T-type Fillet Weld

The residual stresses and their distributions along the welding direction (x) on the surface of a fillet weld computed by three dimensional thermal elastic plastic FEM are shown in Fig. 4. From Fig. 4, it can be observed that the residual stresses distribute uniformly along the welding direction, except those near the two ends of the weld. From this fact, a simplification for 3-dimensional FEM model can be expected when attention is only paid to the residual stresses distributed in the middle transverse section.

In order to simplify the three dimensional FEM analysis, the distribution characteristics of residual strain  $\epsilon_x$  are investigated. The distributions of the residual strain  $\epsilon_x$  in the y and the z directions of the middle transverse section are shown in Figs. 5. From Fig. 5, it can be observed that the longitudinal strain  $\epsilon_x$  distributes linearly in the y-z plane or transverse section of the welded joints.

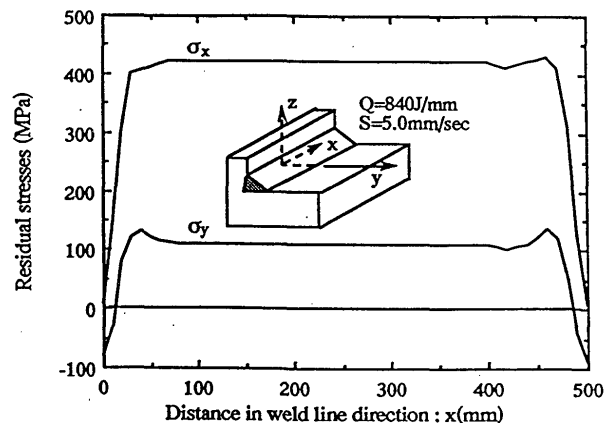


Fig. 4 Residual stresses on the surface of fillet weld and their distributions in welding direction

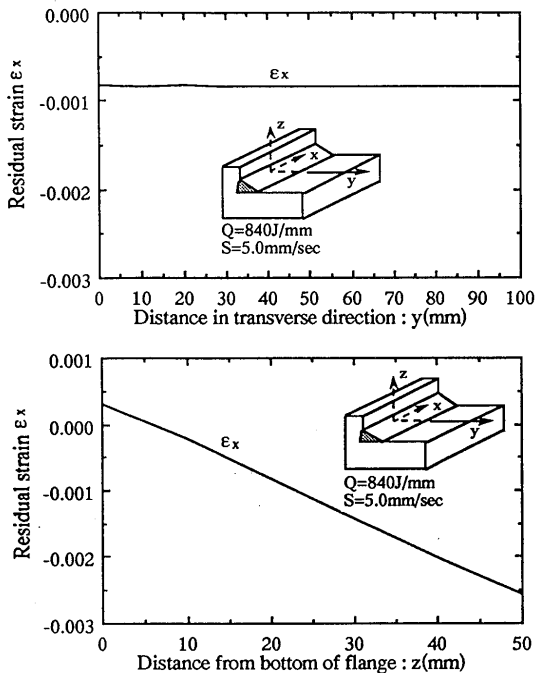


Fig. 5 Longitudinal strain distributions on the middle section of long T-type fillet weld

### 3. Generalized Plane Strain FEM Modelling and Residual Stresses in T-Type Fillet Welds

#### 3.1 Generalized Plane Strain FEM Modelling

If the weld length is assumed to be infinitely long, the transverse section of the welded joint keeps plane when it deforms during welding and after welding. This kind of deformation is called plane deformation or generalized plane strain. If the welding direction is taken as x and the coordinates on the transverse section are taken as y and z, the strain  $\epsilon_x$  distributed in the transverse section can be expressed by the following linear function :

$$\epsilon_x = a_1 + a_2 y + a_3 z$$

Where  $a_1$ ,  $a_2$  and  $a_3$  are the coefficients which can be computed by FEM using the equilibrium equation of force ( $F_x$ ) and moments  $M_y$  and  $M_z$  acting on the transverse section.

With the aid of this generalized plane strain condition, the three dimensional residual stress components  $\sigma_x$ ,  $\sigma_y$ ,  $\sigma_z$  and  $\tau_{yz}$  distributed in the transverse section can be computed by thermal elastic plastic FEM using only the transverse section with unit thickness as a model.

In practical welding, the welding heat source is moving. To simplify the analysis, it is assumed that the welding heat source is simultaneously applied to the weld metal. Therefore, two dimensional welding heat conduction FEM can be employed in the computation of the temperature distribution and thermal cycles.

#### 3.2 Accuracy of Generalized Plane Strain FEM Modelling for Residual Stresses

In order to examine the accuracy of generalized plane strain FEM modelling, the residual stresses are simulated by both generalized plane strain FEM and 3-D FEM

Fig. 6 shows the mesh division and boundary condition used in generalized plane strain FEM. The computed residual stress distributions in the width direction (y) of the flange are shown in Fig. 7. The solid lines and broken lines in Fig. 7 represent the residual stresses computed respectively by 3-D FEM and generalized plane strain FEM. The residual stress distributions computed by generalized plane strain FEM show very good agreement with those by 3-D FEM. The local residual stresses near the weld toe computed by generalized plane strain FEM are slightly larger than those computed by 3-D FEM. This can be explained by the fact that the mesh in generalized plane strain FEM is finer than in 3-D FEM. Because the generalized plane strain FEM shows a good accuracy in the analysis of residual stresses, all the computations which will be presented in the followings are performed by this simple method. The material used in the following computations is assumed to be mild steel.

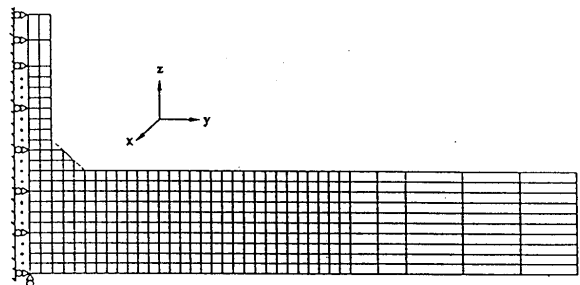


Fig. 6 Mesh division on the transverse section of long T-type fillet weld used in generalized plane strain FEM

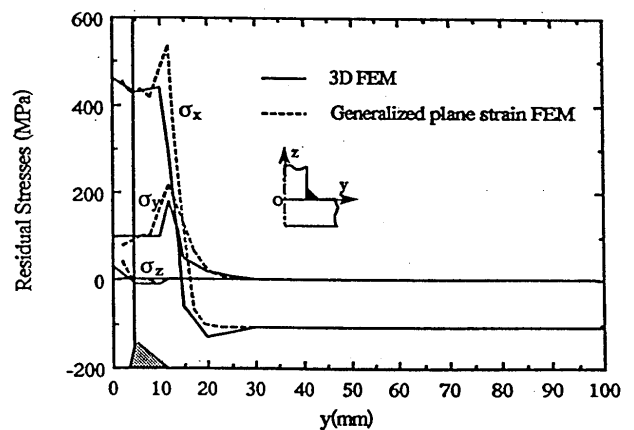


Fig. 7 Residual stresses computed by generalized plane strain FEM

#### 4 Residual Stresses in Single Pass T-type Fillet welds and the Effect of Welding Penetration, Welding Sequence

To investigate the effect of welding penetration and welding sequence, the partial penetration fillet weld shown in Fig. 8(a) and full penetration fillet weld shown in Fig. 8(b) are employed<sup>12)</sup>. The thickness and width of the flange are denoted by  $H_F$  and  $2B_F$ , those of the web are denoted by  $H_W$  and  $B_W$ . For the partial penetration fillet weld, the penetration is expressed by  $p$  which varies from zero (No Penetration) to  $H_W/2$  (Full Penetration) according to the welding conditions.

The sizes of flange and web used in the analysis are  $H_F=16$  mm,  $B_F=100$  mm;  $H_W=12$  mm,  $B_W=100$  mm. The flange and the web with these thicknesses are commonly used in ship structures. The fillet size is 6 mm after welding. The size of the fillet tack weld before the full welding is assumed to be 2 mm. The effective heat input per weld length is assumed to be 610, 850, 1100 and 1300 (J/mm). These heat inputs correspond to the penetration  $p$  of 0, 2, 4 and 6 mm, respectively.

For a T-type fillet joint, the left weld ( $W_1$ ) and right weld ( $W_2$ ) can be welded simultaneously or sequentially. For convenience, these are called simultaneous welding and sequential welding, respectively. In sequential welding, the right weld ( $W_2$ ) is welded after the left weld ( $W_1$ ) is formed and the temperature falls to room temperature. The welding heat input is assumed to be the same for the both welds.

The residual stresses distributed in the transverse direction ( $y$ ) of the flange computed by thermal elastic-plastic FEM are shown for the partial penetration and full penetration single pass T-type fillet welds, in Fig. 9 and Fig. 10, respectively. The solid lines and broken lines in Figs. 9, 10 are the results due to simultaneous welding and sequential welding, respectively.

The longitudinal residual stress  $\sigma_x$  shows trapezoidal shape distribution. Near the fillet welds, a very large tensile residual stress  $\sigma_x$  exists and in the zone away from the welds it becomes a compressive residual stress. The value of the maximum tensile residual stress reaches the yield stress of the material and almost does not change with the welding sequence and penetration. The zone of tensile residual stress  $\sigma_x$  becomes larger in simultaneous full penetration welding.

The distribution of transverse residual stress  $\sigma_y$  is complex compared with residual stress  $\sigma_x$ . A very large tensile residual stress  $\sigma_y$  is produced at the surface of base plates near the fillet weld toes in both simultaneous welding and sequential welding. The value of the tensile transverse residual stress  $\sigma_y$  near the weld toes in partial penetration fillet weld is larger than that in full penetration weld. This may be explained by the fact that the internal restraint in partial penetration fillet weld becomes relatively stronger than that in the full penetration case. In the zone between two fillet welds and

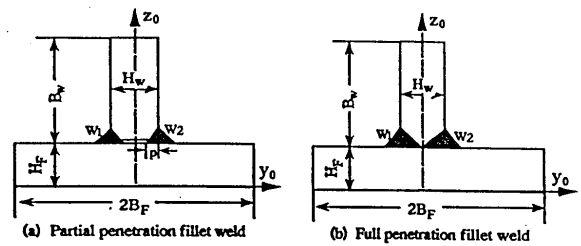


Fig. 8 Partial and full penetration T-type fillet welds

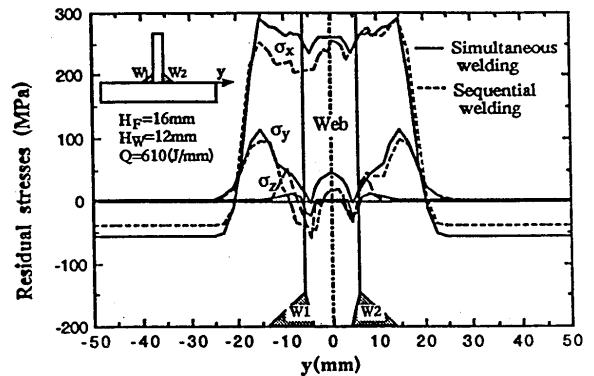


Fig. 9 Residual stresses in partial penetration fillet weld

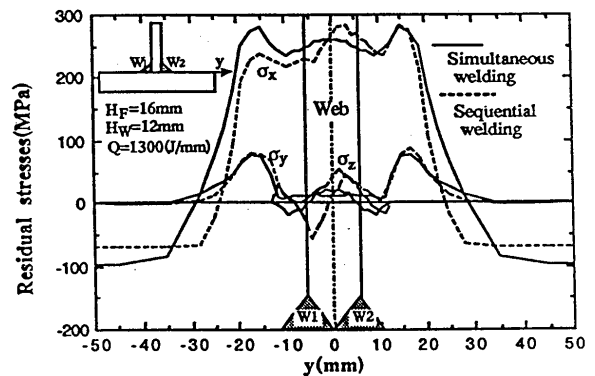


Fig. 10 Residual stresses in full penetration fillet weld

in the left weld metal which is first welded, the local residual stress  $\sigma_y$  varies with the welding sequence and penetration.

#### 5. Residual Stresses in Multipass T-type Fillet Weld

As shown in Fig. 11, the multipass fillet weld is a 3 layer and 5 pass weld whose fillet size is 14 mm. The thickness of flange and web is  $H_F=20$  mm,  $H_W=10$  mm, respectively. Interpass temperature is equal to the room temperature. The effective heat input per weld length for each of 5 weld passes are 630, 630, 630, 720 and 720 (J/mm). The penetration is assumed to be 1 mm.

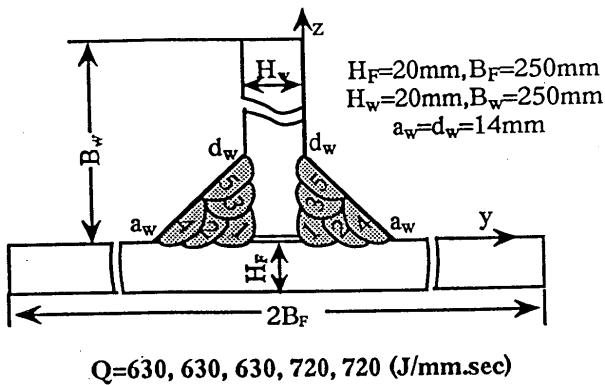


Fig. 11 Multipass T-type fillet weld

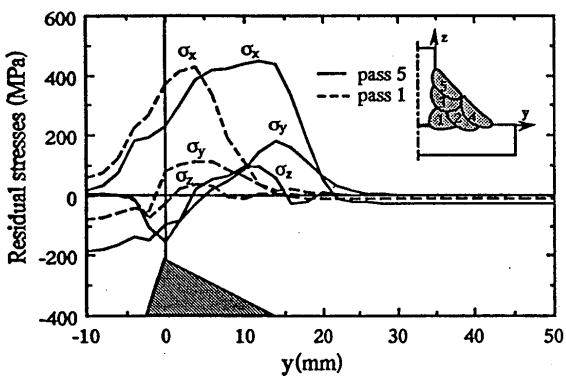


Fig. 12 Residual stresses in multipass fillet weld

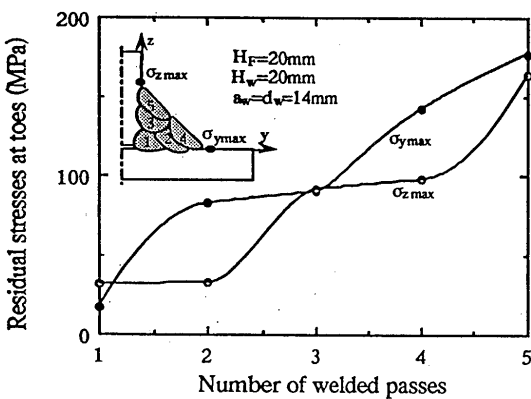


Fig. 13 The change of local residual stresses near the fillet weld toes during multipass welding

The residual stress distributions in transverse direction ( $y$ ) of flange are shown in Fig. 12. The solid lines and broken lines in Fig. 12 show the results of residual stresses due to multipass and single pass welding, respectively. In both multipass welding and single pass welding, the distribution shapes of residual stress are almost similar. In the multipass fillet weld, the maximum tensile residual stresses is produced in the last

weld layer. The tensile transverse stresses  $\sigma_y$  and  $\sigma_z$  in multipass weld toes become larger than those in single pass weld toes. The change of the largest transverse residual stresses  $\sigma_y$  and  $\sigma_z$  with weld passes is shown in Fig. 13. The residual stress  $\sigma_y$  near the toe of flange is small after 1st pass welding. It increases during the 2nd and the 4th pass welding. But it almost does not change with the 3rd pass welding. Similarly, the tensile transverse residual stress  $\sigma_z$  near the toe of the web is small in the 1st and 2nd passes, and it is mainly induced by the 3rd and the 5th pass welding. From these results, it can be observed that the tensile transverse residual stresses  $\sigma_y$  and  $\sigma_z$  near the weld toes are almost determined by the two welding passes close to the toes.

### 6. Residual Stress near Fillet Weld Toe and Its Influencing Factors

The longitudinal residual stress  $\sigma_x$  near the weld toes reaches the yield stress of the material and is rarely affected by welding conditions. The transverse residual stress  $\sigma_y$  is smaller than  $\sigma_x$ , but it has a detrimental effect on fatigue cracking at the toe when a transverse load is applied. Therefore, attention is paid to the tensile transverse residual stress  $\sigma_y$  and the effects of welding penetration, heat input, plate thickness and the restraint condition are investigated in this research.

#### 6.1 Effect of Penetration, Heat Input and Welding Sequence on Residual Stress

The change of the maximum tensile transverse residual stress  $\sigma_{y\max}$  with welding penetration of equivalent heat input for unit weld length is shown in Fig. 14. The solid lines and broken lines in the Fig. 14 show the results in the cases of simultaneous welding and sequential welding. Welding sequence has a very small effect on the transverse residual stresses near the weld toes. Compared with large transverse residual stress  $\sigma_y$  near weld toe of flange, the transverse residual stress  $\sigma_z$

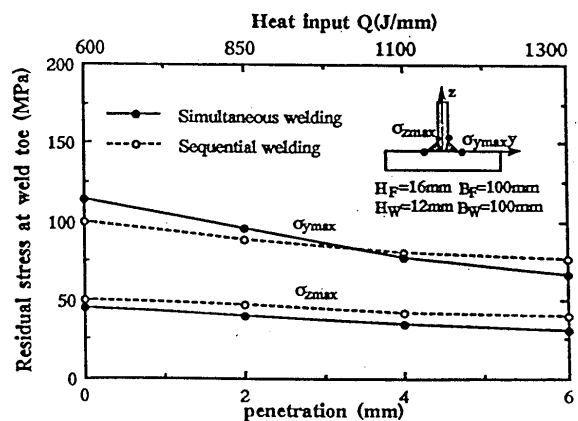


Fig. 14 Effect of welding penetration and heat input on the local residual stresses near fillet weld toes

near the toe of web is quite small. With increasing heat input and welding penetration, the tensile transverse residual stress near the weld toes decreases.

### 6.2 Effect of Flange Thickness on Residual Stress

Figure 15 shows the effect of flange thickness on the maximum tensile transverse residual stress  $\sigma_{y\max}$  near the weld toe of flange. With increasing flange thickness, the internal restraint becomes stronger and residual stress becomes larger.

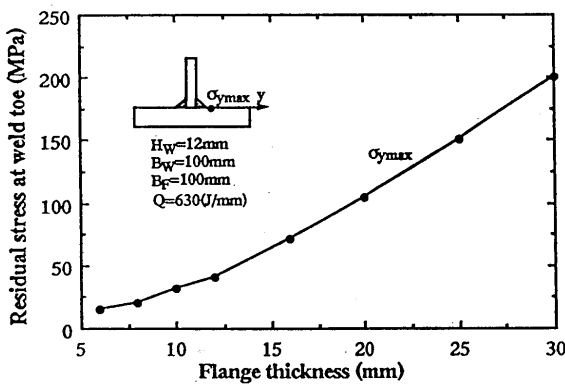


Fig. 15 Effect of flange thickness on the local residual stress near the fillet weld toe

### 6.3 Effect of Restraint Conditions on Residual Stress

In fillet welding, to reduce the angular distortion a restraint is applied to the flange as shown in Fig. 16 and after welding the restraint is removed. In this research, the residual stresses in the restrained fillet joint is simulated by thermal elastic-plastic FEM. In the computation, the restraint position is selected on elastic-plastic deformation boundary due to welding because this position is most efficient for the prevention of angular distortion, which will be described later.

The computed residual stress distributions in the y direction are shown in Fig. 17. The solid line, broken line and dashed line in Fig. 17 show the residual stresses, respectively, in unrestrained fillet weld, in the fillet weld under restraint state and in the fillet weld after the restraint force is released. From Fig. 17, it can be observed that residual stress and its distribution in the unrestrained fillet weld and in fillet weld under restraint state is almost the same. When the restraint is removed after welding, the flange is slightly bent by the released restraint force, and then the compressive transverse stress on the top surface of flange and the tensile transverse stress on the bottom surface of flange are induced. Therefore the tensile transverse stress near the toe is reduced. This means that the restraint used to prevent angular distortion is also effective in reducing the tensile transverse residual stress near the weld toe.

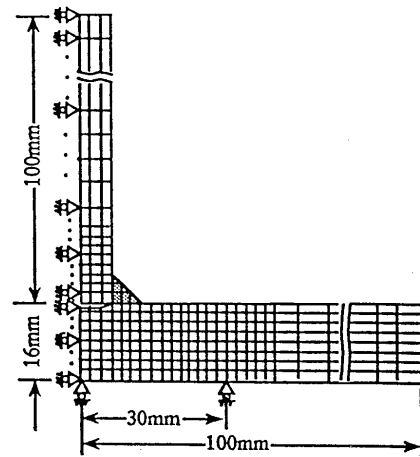


Fig. 16 Restraint condition in T-type fillet welding

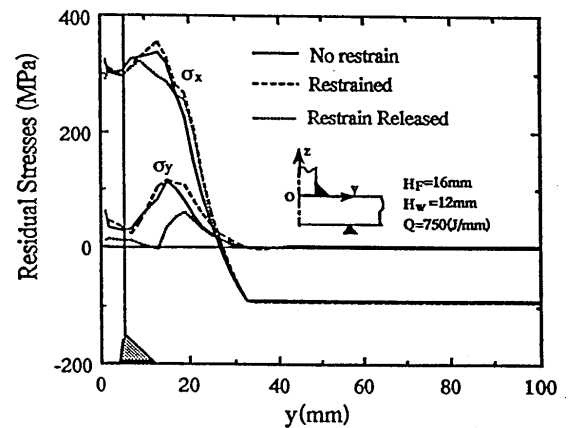


Fig. 17 Effect of restraint conditions on residual stresses in fillet welds

## 7 Angular Distortion in T-type Fillet Welds and The Effect of Welding Conditions

### 7.1 Angular Distortion of T-type Fillet Welds

The deformation of T-type fillet welds includes longitudinal shrinkage, transverse shrinkage, longitudinal bending and angular distortion. In this paper, the attention is only paid to the angular distortion. As shown in Fig. 18, the angular distortion in flange and web is denoted by  $\theta_F$  and  $\theta_W$  respectively.

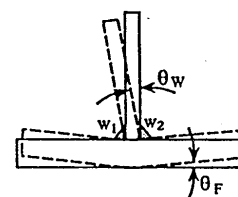


Fig. 18 Schematic showing of angular distortion in T-type fillet welds

### 7.2 Effect of Welding Sequence on Angular Distortion

In the partial penetration T-type fillet welding, the changes of angular distortion ( $\theta_F$ ) of flange and that ( $\theta_W$ ) of web, with time, computed by generalized plane strain FEM, are shown in Fig. 19. The change tendency of angular distortion ( $\theta_F$ ) of flange with time in sequence welding is similar with that in simultaneous welding. The summation of angular distortion ( $\theta_{F1} + \theta_{F2}$ ) due to left fillet weld (W1) and right fillet weld (W2) in sequence welding is approximately equal to the angular distortion in simultaneous welding. The angular distortion  $\theta_{W1}$  of web due the first fillet weld (W1) and that  $\theta_{W2}$  due to the second fillet weld (W2) are just opposite in their change tendency with time. The angular distortion due to first fillet weld is larger than that due to the second fillet weld because the stiffness is small in the first fillet welding. Therefore, the residual angular distortion ( $\theta_{W1} + \theta_{W2}$ ) makes the web bends into the first welded side.

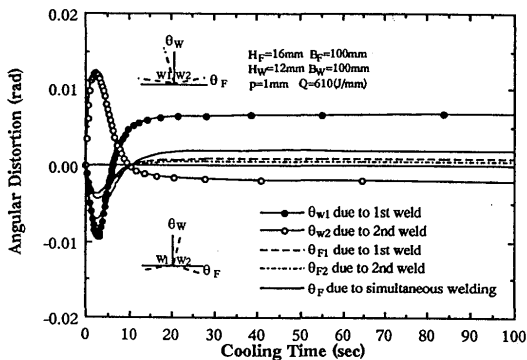


Fig. 19 Angular distortion of T-type fillet welds in simultaneous and sequence welding

### 7.3 Effect of Working table on Angular Distortion

In the actual T-type fillet welding, the flange is often supported by a working table. The working table resists the deflection of the flange toward to it but no restraint for the deflection backward to it. To simulate this restraint condition of the working table, contactable spring elements are introduced as shown in Fig. 20. When the spring elements are compressed or strain is compressive, the spring elements have very big stiffness and the flange is rigidly supported by spring elements. when strain in spring elements is tensile, the stiffness of spring elements will become very small and the flange will deflect freely.

Fig. 21 shows the angular distortion changes with time computed by generalized plane strain FEM when the flange is completely free and rigidly supported by the working table. The residual angular distortion of the

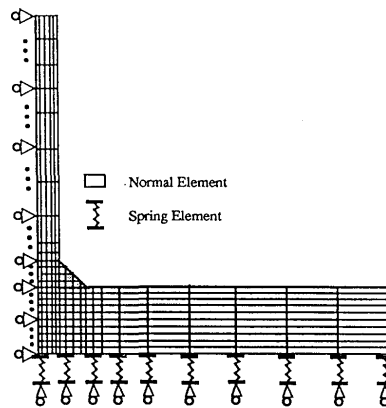


Fig. 20 Simulation of restrain of working table by contactable spring elements

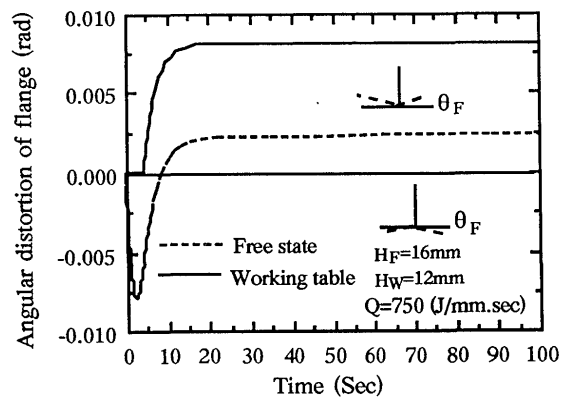


Fig. 21 Effect of restrain of working table on angular distortion of flange of T-type fillet weld

flange supported by the working table during welding is much larger than that in the free state. From Fig. 21, it can be observed that the negative angular distortion of flange in the welding of free T-type fillet welds is almost transformed into the positive residual angular distortion when the restraint of the working table is considered in the FEM simulation.

### 7.4 Effect of Applied Restraint Position on Angular Distortion

In order to reduce the angular distortion, external restraint is often applied in production, shown in Fig. 16. However, how to select the restraint position become a very important problem. In this research, the restraint position applied to the flange is changed, and the position effect on the angular distortion due to welding and the restraint force releasing is simulated by generalized plane strain thermal elastic plastic FEM and elastic plastic FEM, respectively. When the applied restraint is removed after welding, the computed residual angular distortion of flange is shown in Fig. 22. It can be observed from Fig. 22 that the residual angular distortion is much reduced compared with the angular distortion when the flange is supported by a rigid working



table. When the applied restraint position is selected at the elastic-plastic deformation boundary, a minimum angular distortion can be obtained according to this computation.

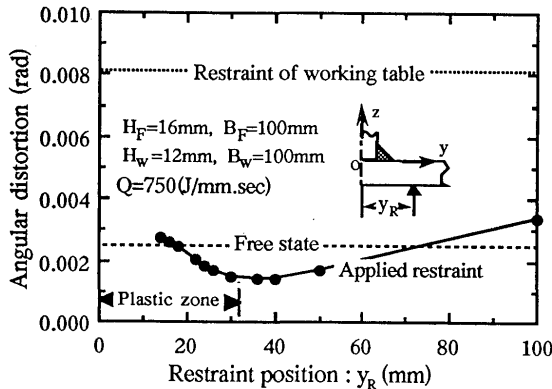


Fig. 22 Effect of applied restraint position on the residual angular distortion

### 8 Conclusions

In this paper, the three dimensional residual stresses and angular distortion in T-type fillet welds are simulated by thermal elastic plastic 3-D FEM, and generalized plane strain FEM in which the mesh division is only made on the transverse section. The main conclusions are as follows:

- (1) The generalized plane strain FEM has a good accuracy in the analysis of three dimensional residual stresses distributed in the transverse sections compared with those computed by 3-D FEM.
- (2) The residual stress has a similar distribution pattern in both one pass and multipass T-type fillet welds.
- (3) Welding sequence has little effect on the welding residual stress distributions except for the local stresses near the first fillet welded metal.
- (4) A large tensile transverse residual stress is produced near the fillet weld toe.
- (5) The maximum tensile transverse residual stress near multipass fillet weld toes is larger than that in one pass fillet welds, and it is mainly induced by the two welding passes close to the fillet toe.
- (6) With increasing penetration or heat input in fillet welding, the tensile transverse residual stress near the fillet weld toe decreases.
- (7) With increasing flange thickness, the tensile transverse residual stress near the fillet weld toe increases.
- (8) In a restrained fillet weld, the tensile transverse residual stress near the fillet weld toe can be reduced after the restraint force is released.
- (9) Welding sequence has very large effect on angular distortion of web and less effect on that of flange in T-type fillet welds.

- (10) The support of working table has very large effect on the angular distortion of flange.
- (11) When the external restraint is applied to the position of elastic-plastic boundary, the residual angular distortion can be reduced to be minimum.

### References

- (1) Y. Ueda, K. Nakacho: Simplifying Method for Analysis of Transient and residual Stresses and Deformations due to multipass Welding, Trans. of Welding Research Institute of Osaka University (JWRI), Vol. 11 (1982) No. 1, p. 95-103
- (2) Y. Ueda and T. Yamakawa: Analysis of Thermal Elastic-Plastic stress and Strain during Welding by Finite Element Method, Trans. Japan Welding Soc. (JWS) Vol.2 (1971) No.1, p. 90-100
- (3) R.I. Karlsson and B.L. Josefson: Three-Dimensional Finite Element Analysis of Temperature and Stresses in a Single-Pass Butt Welded Pipe, Trans. ASME, Journal of Pressure Vessel Technology, Vol. 112, Feb. 1990, P. 76-84
- (4) J.A. Goldak et al: A new Finite Element Model for Welding Heat Sources, Trans. AIME, Vol.15B, June 1984, P. 299-305
- (5) R.H. Reggatt: Residual Stresses and Distortion in Multipass Butt Welded Joints in Type 316 Stainless Steel, Int. Conf. on Residual Stresses in Science and Technology, Ed. E. Macherauch & V. Haunk, Deutsche Gessellschaft, Oberursel, FRG, 1987
- (6) S. Brown and H. Song: Implications of Three Dimensional Numerical Simulations of Welding of Large Structures, Welding Journal, Vol. 71, 1992, No.2, P. 55-62
- (7) W. Cheng and I. Finnie: Measurement of Residual Stress Distributions near the toe of a Weld between a Bracket and a Plate Using the Crack Compliance Method, Proc. IUTAM Symposium on Mechanical Effects of Welding, Lulea, Sweden, 2-6, June, 1991, Ed. L. Karlson, Pub. Springer-Verlag Berlin Heidelberg, 1992
- (8) Y. Ueda and M.G. Yuan: Prediction of Residual Stresses in T- and I-Joints Using Inherent strains, Trans. JWRI, Vol.22 (1993), No. 1, p. 157-168
- (9) Y. Ueda and N.X. Ma : Function Expression for Inherent strains in Fillet Welds and Its Accuracy. Quartely Journal of Japan Welding Society, Vol. 12 (1994) No. 4, p. 555-560
- (10) K. Ohji: Fatigue Crack Propagation in Residual Stress Field, third Int. Conf. on Residual Stresses, Tokushima, Japan, 23-26 July, 1991, Residual Stresses III, Ed. H. Fujiwara et al, Elsevier Applied Science, p.447-456
- (11) O. Watanabe et al: Fatigue Strength of Welded Joint of High Strength Steel and Its Controlling Factor, Quartely Journal of Japan Welding Society, Vol. 13 (1995) No. 3, p. 438-443
- (12) N.X. Ma and Y. Ueda : FEM Analysis for The Effect of Welding Conditions on Deformation and Residual Stresses of T-type Fillet Welds, Preprints of The National Meeting of Japan Welding Society, Tokyo, Japan, No. 56, 1995, p. 140-141